

Quantum distillation: dynamical generation of low-entropy states of strongly correlated fermions in an optical lattice

F. Heidrich-Meisner,¹ S. R. Manmana,² M. Rigol,³ A. Muramatsu,⁴ A. E. Feiguin,^{5,6,7} and E. Dagotto⁸

¹*Institut für Theoretische Physik C, RWTH Aachen University, 52056 Aachen, Germany*

²*Institute of Theoretical Physics, École Polytechnique Fédérale de Lausanne, CH-1015 Lausanne, Switzerland*

³*Department of Physics, Georgetown University, Washington, District of Columbia 20057, USA*

⁴*Institut für Theoretische Physik III, Universität Stuttgart, 70550 Stuttgart, Germany*

⁵*Department of Physics and Astronomy, University of Wyoming, Laramie, WY 82071, USA*

⁶*Microsoft Project Q, University of California, Santa Barbara, CA 93106, USA*

⁷*Condensed Matter Theory Center, University of Maryland, College Park, MD 20742, USA*

⁸*Materials Science and Technology Division, Oak Ridge National Laboratory, Oak Ridge, Tennessee 37831, USA and Department of Physics and Astronomy, University of Tennessee, Knoxville, Tennessee 37996, USA*

(Dated: October 19, 2009)

Correlations between particles can lead to subtle and sometimes counterintuitive phenomena. We analyze one such case, occurring during the sudden expansion of fermions in a lattice when the initial state has a strong admixture of double occupancies. We promote the notion of quantum distillation: during the expansion, and in the case of strongly repulsive interactions, doublons group together, forming a nearly ideal band insulator, which is metastable with a low entropy. We propose that this effect could be used for cooling purposes in experiments with two-component Fermi gases.

One of the most exciting features about ultracold atom gases is the possibility of experimentally studying strongly correlated systems with time-dependent interactions and in out-of-equilibrium situations (for a review, see [1]). For instance, a time-dependent tuning of parameters has been used to illustrate the collapse and revival of coherence properties of bosons in an optical lattice suggested to be well described by the Bose-Hubbard model [2]. Also, the question of the relaxation of strongly correlated systems initially prepared in a high-energy state that typically is not an eigenstate has been studied [3], as well as the intimately related question of thermalization [4]. A third context is the expansion of originally trapped particles into an empty optical lattice or a waveguide.

While expansions after turning off all trapping potentials and lattices are commonly used to measure the momentum distribution of the originally trapped system [1], recently, several studies have investigated the expansion in one dimensional (1D) geometries with and without the presence of an optical lattice along the 1D tubes. In 1D cases, in contrast to the usual time-of-flight experiments, interactions play a fundamental role. The findings include phenomena such as the fermionization of the momentum distribution function of hard-core bosons and anyons [5], the asymptotic transformation of generic Lieb-Liniger wave-functions to a Tonks-Girardeau structure [6], the emergence of quasi-coherence in bosonic [7] and fermionic systems [8], or disorder-induced effects [9]. Such expansions have already experimentally been realized in 1D ultracold atomic gases [10].

While strongly correlated phases of bosons in optical lattices have been observed and studied in many experiments, reaching the quantum degenerate regime of fermions is more difficult [1, 11]. Only recently, evidence for the observation of the Mott-insulator (MI) transition of a two-component Fermi gas in optical lattices has been presented [12]. Unfortunately, the temperatures in those

experiments are still too high to observe the expected low-temperature insulating antiferromagnetic phase, and to make contact with the regime of interest to high- T_c superconductivity [13]. Hence, intense efforts are currently under way to develop efficient cooling schemes for fermions in optical lattices [14].

In this Rapid Communication, we study the expansion of a two-component Fermi gas in an optical lattice from an initial state with a strong admixture of doubly occupied sites. Our main result is the observation that double occupancies (doublons) are dynamically separated from the rest of the system and that they group together into a metastable state, which is very close to a Fock state. The condition for this to happen is that interaction energies need to be much larger than the kinetic energy. Our results are in qualitative agreement with recent studies that have argued, invoking a similar reasoning, that relaxation times can be rather long, and one may thus encounter metastable states (see, *e.g.*, Ref. [15]). Experimentally, this phenomenon has been observed as repulsively bound pairs in the case of bosons [16]. We will also discuss the potential of our findings as a cooling technique where one dynamically generates a low-entropy region in a system with arbitrarily large values of the on-site repulsion.

Model and methods – We consider the one-dimensional (1D) Hubbard model:

$$H_0 = -t \sum_{i=1}^{L-1} (c_{i+1,\sigma}^\dagger c_{i,\sigma} + \text{h.c.}) + U \sum_{i=1}^L n_{i,\uparrow} n_{i,\downarrow}. \quad (1)$$

Standard definitions are employed in Eq. (1) [8]. Open boundary conditions are imposed, L is the number of sites and N the number of particles (with a filling factor $n = N/L$). The nonequilibrium dynamics is studied using the adaptive time-dependent density matrix renormalization group method (tDMRG) [17] and time-dependent exact diagonalization (ED) techniques [18].

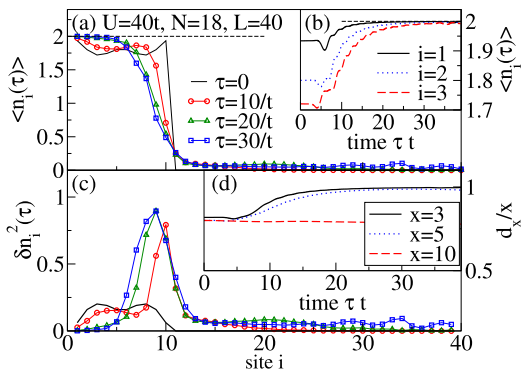


FIG. 1: (Color online) Expansion from an initial state with $n_{\text{init}} = 1.8$ ($N = 18$, $U = 40t$): (a) Density $\langle n_i(\tau) \rangle$ and (c) local charge fluctuations δn_i^2 for times $\tau t = 0, 10, 20, 30$. Insets: (b): $\langle n_i(\tau) \rangle$ vs time for $i = 1, 2, 3$. (d) Average double occupancy $d_x(\tau)/x$ for $x = 3, 5, 10$ ($d_x(\tau) = \sum_{i=0}^x \langle \tilde{d}_i(\tau) \rangle$).

We prepare initial states with particles confined into a finite region of an optical lattice, with a filling factor of $1 < n_{\text{init}} < 2$ in that region and zero otherwise. To this end [8], we apply onsite energies ϵ_i to only a portion of the system: $H_{\text{conf}} = \sum_{i=1}^L \epsilon_i n_i$ ($\epsilon_i \sim 10^6 t$ for $1 < i_0 < i \leq L$ and $\epsilon_i = 0$ elsewhere). Hence, at time $\tau \leq 0$, we have $H = H_0 + H_{\text{conf}}$, while we turn off H_{conf} at $\tau = 0^+$. In our tDMRG runs, we use either a third-order Trotter-Suzuki time-evolution scheme or a Krylov-space based method [18], with time steps of $\delta\tau t = 0.01$ and 0.005 (we set $\hbar = 1$). During the time-evolution, we keep up to 1600 states.

Results – Figure 1(a) shows snapshots of density profiles $\langle n_i(\tau) \rangle$ at several times for $U = 40t$ and $n_{\text{init}} = 1.8$ (for results for other n_{init} , see [19]). Since $U \gg 4t$, single-particle hopping can only propagate a particle out of a doubly occupied site into the empty sites to the right of the initially occupied region if, at the same time, the remaining particle is moved to the left into a site that was previously singly occupied, in order to preserve the total energy. For that reason, the density in the first sites *increases* as the remaining of the block slowly “melts”. From Fig. 1(b), one can see that the density in the first sites gets very close to $\langle n_i \rangle = 2$, which promotes the picture that dynamically, doublons are separated from the rest and group together in a region of the lattice.

We introduce the term quantum distillation for this process. Figure 1(c) shows the local charge fluctuations $\delta n_i^2 = \langle n_i^2 \rangle - \langle n_i \rangle^2$. Consistent with the picture described before, these fluctuations are the largest in the interface region (sites 7-11 in the figure), while they die out in the first sites as time increases. To gain a better understanding of how this happens with time, we compute the average double occupancy d_x/x ($d_x = \sum_{i=0}^x \langle \tilde{d}_i(\tau) \rangle$; $\tilde{d}_i = n_{i\uparrow} n_{i\downarrow}$) on the x first sites, counting from the left. Figure 1(d) depicts this quantity for different values of x . For $x < 10$ and, e.g., $x = 3, 5$, the average double occupancy increases towards $d_x/x = 1$, which is quite stable

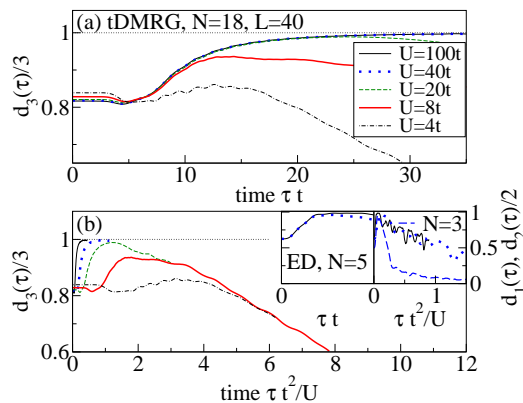


FIG. 2: (Color online) Average double occupancy $d_3(\tau)/3$ ($n_{\text{init}} = 1.8$): vs (a) time τ and (b) vs $\tau t^2/U$ for $U/t = 4, 8, 20, 40, 100$ (tDMRG). Insets in (b): d_1 for $N = 5$ ($U/t = 40, 100$); $d_2/2$ for $N = 3$ ($U = 40t$, thin dashed line) (ED).

over a long time window for $U \geq 40t$ [Fig. 1(d)]. For $x = 10$, i.e., the block with $\langle n_i \rangle > 0$ at $\tau = 0$, this quantity remains almost constant: this is basically equivalent to saying that only a small portion of the interaction energy $E_{\text{int}} = U \sum_{i=1}^{10} \langle \tilde{d}_i \rangle$ is converted into kinetic energy during the times simulated.

Time scales – We next address the question on which time scales (i) the Fock state is formed and (ii) it decays. The latter is equivalent to asking on what time scale a band insulator (BI) in the large U limit would decay. While from energy considerations it is clear that a piece of doubly occupied sites, i.e., a BI, delocalizes on a time-scale of U/t^2 [16], we are primarily interested in the case of $1 < n_{\text{init}} < 2$. To address this situation, we first perform ED calculations for a short initial state with $1 < n_{\text{init}} < 2$, specifically $N = 3, 5$ on two and three sites, respectively [see the insets of Fig. 2(b)]. In this case, one can clearly see that doublons form on the first sites on a U -independent time-scale, governed by the bare hopping matrix element t . Doublons then get delocalized over the neighboring empty sites on a time-scale U/t^2 (times a prefactor that scales with N), consistent with the decay-rate of a BI.

Our tDMRG results presented in Figs. 2(a) and (b) unveil that the same picture holds for $n = 1.8$ with $N = 18$. Figure 2(a) shows the average double occupancy on the first three sites for several values of U . Quantum distillation is best realized for $U > 8t$ (as opposed to $U \lesssim 8t$), since, at $U = 8t$, the average double occupancy increases with time ($\tau > 5/t$), but it reaches a maximum value that is well below one. Nevertheless, as the large- U results show, the formation of a quasi-Fock state happens over a U -independent time-scale. Figure 2(b) displays the same data versus $\tau t^2/U$, and the small- U curves fall on top of each other at times $\tau t^2/U > 4$, while the large- U data seem to approach the same curve, too. The results of Fig. 2(b) show, in the example of $x = 3$, that the Fock state will start to delocalize after a time $\tau \sim 50/t$ in the $U = 40t$ case ($\tau \sim 120/t$ for $U = 100t$).

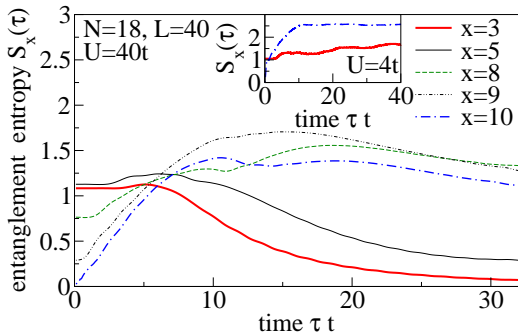


FIG. 3: (Color online) Entanglement entropy S_x ($n_{\text{init}} = 1.8$, $U = 40t$). Inset: S_x for $x = 3, 10$ at $U = 4t$.

While we have presented results for $N = 18$, the physics does not qualitatively change upon increasing N at a fixed n_{init} [19]. Essentially, the time scale for building up the Fock state scales linearly with N [19]. Note that in typical experiments with 1D optical lattices, on the order of 100 atoms are confined in one 1D structure [1]. It should be readily possible to experimentally observe the quantum distillation by measuring, *e.g.*, the radius R_d of the double occupancies [$R_d^2(\tau) \propto \sum_i \langle \hat{d}_i(\tau) \rangle^2$, see [19]]. We predict that, for $U \gg 4t$ and $n_{\text{init}} > 1$, this quantity should decrease as a function of time. As U/t depends exponentially on the lattice depth V_0 , one can enter into the regime $U \gg 4t$ by tuning V_0 [20].

Entanglement entropy – Further quantitative information can be gained by invoking the entanglement entropy $S_x = -\text{tr}[\rho \ln(\rho)]$ (Ref. [21]), where ρ is the reduced density matrix of a subsystem of length x [22]. The subsystems of primary interest here are those where double occupancy increases as time evolves, as illustrated in Fig. 1(d) (x counts the sites starting from the left end).

Figure 3 depicts one of our most important results, constituting a defining property of the quantum distillation process, namely, the spontaneous reduction of the entanglement entropy in the metastable region where doublons group together. We plot S_x for several $x \leq 10$ at $U = 40t$, which ought to be contrasted against the corresponding $U = 4t$ data, shown in the inset. Figure 3 shows that for the leftmost sites, $S_x(\tau = 0)$ is nonzero and remains approximately constant for some x -dependent time window (*e.g.*, $\tau t \lesssim 5$ for $x = 3$). At later times, the behavior strongly depends on the value of U/t . For $U/t = 4$, S_3 increases as the density decreases, while for $U/t = 40$, S_3 decreases, on the time scales simulated, by a factor of 15 as the metastable state with $\langle n_i \rangle = 2$ is generated. We relate this decrease of S_x to the quantum distillation, which creates regions with low entanglement. This is complementary to experiments aiming at preparing maximally entangled states [23].

Harmonic trap – While there are experimental efforts directed at engineering box-like traps (see, *e.g.*, Ref. [24]), which is the case our results presented so far directly apply to, in most typical experiments with optical lattices, the atoms experience a harmonic confinement [1]. We

now consider this case to show that quantum distillation works even in the more difficult case of strongly inhomogeneous initial states, using $H_{\text{conf}} = V_{\text{trap}} \sum_{i=1}^L (i-1)^2 n_i$, where V_{trap} is the curvature of the harmonic potential. The confinement gives rise to a shell structure in the fermionic density [25]: metallic and MI shells alternate, depending on the characteristic density $\bar{\rho} = N \sqrt{V_{\text{trap}}/t}$ [25]. In order to achieve optimal distillation and thus the formation of a low-entropy region, one does not need to follow the approach often discussed in the literature (see, *e.g.*, Ref. [14]), in which U/t is increased adiabatically. Instead, we propose that one can start with a trapped system with a low value of $U/t = 2$. In such cases, double occupancy is energetically favorable against trapping energy and hence ideal for our distillation scheme, and moreover, the presence of MI shells is suppressed. At time $\tau = 0$, one can then quench U/t to a large value [20] and turn off the trapping potential, but keeping the optical lattice on. In many experiments, the trapping potential is provided by the same lasers that produce the lattice, which, however, is not necessary. In order for our scheme to work, one needs a trapping potential that can be controlled independently of the lattice [10].

The tDMRG results for the time-evolution of the quench described above are displayed in Fig. 4. We have taken the final values of U/t after the quench to be $U = 40t$ [Fig. 4(a)] and $U = U_{\text{init}}$ [Fig. 4(b)]. Both figures show the average double occupancy $d_x(\tau)/x$ for several values of x . In Fig. 4(a), one can see that $d_x(\tau)/x$ first decreases and then increases to form the quasi-Fock state. It is also illustrative to compare the initial density profile to one at later times [inset of Fig. 4(b)]: while fast particles escape, a block of particles remains in the initial region of the system. A very different behavior of d_x can be seen in Fig. 4(b). There, since the final value of U/t is small, the system simply melts and no signature of quantum distillation is seen.

During the expansion, the entanglement growth [26] induced by the quench from $U = 2t$ to $40t$ competes with the reduction of the entanglement entropy S_x of blocks with an increasing double occupancy due to the quantum distillation. It is thus an amazing result that, at sufficiently long times and despite the large final value of U chosen in the quench, the quantum distillation wins, as is shown in Fig. 4(c). There, we display S_x for $x = 2, 3, 4$, and indeed, these S_x first increase due to the quench, but eventually drop below their initial value (dotted lines) at the maximum times simulated. For the time-scales considered in Fig. 4(c), we find that $S_2(\tau) \lesssim 0.25 S_2(\tau = 0)$. The same behavior emerges for other values of $\bar{\rho}$, U_{init} , and U [19].

So far, our results suggest that quantum distillation is robust against a variation of initial conditions and quenches. We envision it as a way to experimentally achieve very low temperatures in fermionic systems by creating a very low entropy band insulating state with arbitrarily large values of U/t . Once such a state is created, it can be used as an initial state to achieve an

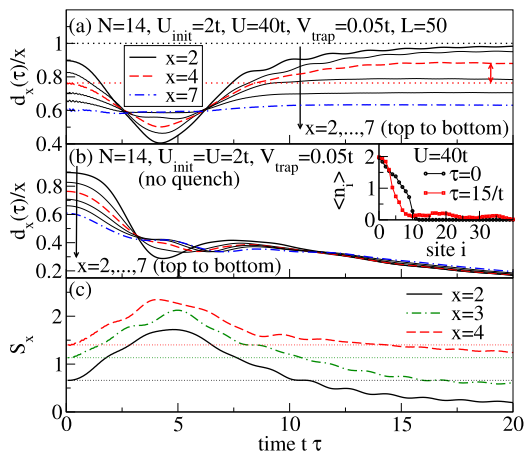


FIG. 4: (Color online) Average double occupancy d_x/x during the expansion from a harmonic trap ($V_{\text{trap}} = 0.05t$, $U_{\text{init}} = 2t$, $N = 14$, $x = 2, 3, \dots, 7$) with (a) a quench to $U = 40t$ and (b) no quench. Dotted line in (a): $d_{x=4}(\tau = 0)$. Inset in (b): density profile at $\tau t = 0, 15$. (c) Entanglement entropy S_x for $x = 2, 3, 4$ ($U = 40t$); horizontal lines are $S_x(\tau = 0)$.

tiferromagnetic MI with one particle per site. The idea would be to load such a BI in a trap for which that state is close to the ground state. This step is important in ensuring a low-entropy initial state that is in equilibrium [27]. One can then adiabatically reduce the strength of

that trapping potential and of the ratio U/t . That way one could produce a final low temperature Mott insulating state starting from a BI.

In conclusion, we demonstrated that low-entropy states of two-component Fermi gases can be dynamically created in optical lattices utilizing the expansion of particles into the empty lattice in the limit of strong interactions. After having the low entropy state in an appropriate trap, an adiabatic lowering of trapping potential and interaction strength can lead to a final low temperature MI. We stress that the quantum distillation we discussed here for fermions will also work in the bosonic case.

Acknowledgments

We thank L. Hackermüller, G. Refael, A. Rosch, U. Schneider, and D. S. Weiss for fruitful discussions. M.R. was supported by startup funds from Georgetown University and by the US Office of Naval Research. A.M. acknowledges partial support by the DFG through SFB/TRR21. E.D. was supported in part by the NSF grant DMR-0706020 and the Division of Materials Science and Engineering, U.S. DOE, under contract with UT-Battelle, LLC. M.R. and A.M. are grateful to the Aspen Center for Physics for its hospitality.

-
- [1] I. Bloch, J. Dalibard, and W. Zwerger, *Rev. Mod. Phys.* **80**, 885 (2008).
[2] M. Greiner *et al.*, *Nature (London)* **419**, 51 (2002).
[3] S. Fölling *et al.* *Nature (London)* **448**, 1029 (2007).
[4] T. Kinoshita, T. Wenger, and D. S. Weiss, *Nature (London)* **440**, 900 (2006); S. Hofferberth *et al.*, *ibid.* **449**, 324 (2007).
[5] M. Rigol and A. Muramatsu, *Phys. Rev. Lett.* **94**, 240403 (2005); A. Minguzzi and D. M. Gangardt, *ibid.* **94**, 240404 (2005); A. del Campo, *Phys. Rev. A* **78**, 045602 (2008).
[6] H. Buljan, R. Pezer, and T. Gasenzer, *Phys. Rev. Lett.* **100**, 080406 (2008); D. Jukić *et al.*, *Phys. Rev. A* **78**, 053602 (2008); D. Jukić, B. Klajn, and H. Buljan, *ibid.* **79**, 033612 (2009).
[7] M. Rigol and A. Muramatsu, *Phys. Rev. Lett.* **93**, 230404 (2004); *Mod. Phys. Lett. B* **19**, 861 (2005); K. Rodriguez *et al.*, *New J. Phys.* **8**, 169 (2006).
[8] F. Heidrich-Meisner *et al.*, *Phys. Rev. A* **78**, 013620 (2008).
[9] B. Horstmann, J.I. Cirac, and T. Roscilde, *Phys. Rev. A* **76**, 043625 (2007); G. Roux *et al.*, *ibid.* **78**, 023628 (2008).
[10] T. Kinoshita, T. Wenger, and D. S. Weiss, *Science* **305**, 1125 (2004); D. Clément *et al.*, *Phys. Rev. Lett.* **95**, 170409 (2005); C. Fort *et al.*, *ibid.* **95**, 170410 (2005).
[11] W. Ketterle and M. W. Zwierlein, arXiv:0801.2500.
[12] R. Jördens *et al.*, *Nature (London)* **455**, 204 (2008); U. Schneider *et al.*, *Science* **322**, 1520 (2008).
[13] W. Hofstetter *et al.*, *Phys. Rev. Lett.* **89**, 220407 (2002).
[14] T.-L. Ho and Q. Zhou, *Proc. Natl. Acad. Sci. U.S.A* **106**, 6916 (2009); J.-S. Bernier *et al.*, *Phys. Rev. A* **79**, 061601(R) (2009).
[15] A. Rosch *et al.*, *Phys. Rev. Lett.* **101**, 265301 (2008).
[16] K. Winkler *et al.*, *Nature (London)* **441**, 853 (2006).
[17] S. R. White and A. E. Feiguin, *Phys. Rev. Lett.* **93**, 076401 (2004); A. Daley *et al.*, *J. Stat. Mech.: Theory Exp.*, P04005 (2004).
[18] S. R. Manmana, A. Muramatsu, and R. M. Noack, *AIP Conf. Proc.* **789**, 269 (2005) and references therein.
[19] See EPAPS Document No. xxx for additional figures. For more information on EPAPS, see <http://www.aip.org/pubservs/epaps.html>
[20] In experiments, U/t should not be too large to avoid the population of higher bands.
[21] See, *e.g.*, A. Polkovnikov, arXiv:0806.2862 and references therein.
[22] U. Schollwöck, *Rev. Mod. Phys.* **77**, 259 (2005).
[23] P. Kwiat *et al.*, *Nature (London)* **409**, 1014 (2001).
[24] T.P. Meyrath *et al.*, *Phys. Rev. A* **71**, 041604(R) (2005).
[25] M. Rigol and A. Muramatsu, *Phys. Rev. A* **69**, 053612 (2004); *Opt. Commun.* **243**, 33 (2004).
[26] P. Calabrese and J. Cardy, *J. Stat. Mech.: Theory Exp.*, P06008 (2007); G. D. Chiara *et al.*, *ibid.*, P03001 (2006).
[27] D. S. Weiss (private communication).

**ELECTRONIC PHYSICS AUXILIARY
PUBLICATION SERVICE FOR: QUANTUM
DISTILLATION: DYNAMICAL GENERATION
OF LOW-ENTROPY STATES OF STRONGLY
CORRELATED FERMIONS IN AN OPTICAL
LATTICE**

**Expansion from a box trap: dependence on the
initial filling n_{init}**

In the main text, we have mostly discussed and presented results for an initial filling of $n_{\text{init}} = 1.8$ with $N = 18$. Here we present additional material for $n_{\text{init}} = 1.2, 1.4, 1.6$ (and, for comparison, the $n_{\text{init}} = 1.8$ data from the main text) to elucidate the dependence of the quantum distillation on n_{init} . Such data are presented for $U/t = 8, 20, 40, 100$ in Figs. 5-8, respectively.

We find that for all $n_{\text{init}} > 1$ and all values of U considered here, quantum distillation takes place. We distinguish between the quantum distillation in a *weak* sense, namely for some sites $\langle n_i(\tau) \rangle > \langle n_i(\tau = 0) \rangle$. Such behavior is seen in the case of $U = 8t$ (Fig. 5). The more pronounced effect of the formation of approximate Fock states, *i.e.*, $\langle n_i(\tau) \rangle \approx 2$, is observed for large n_{init} and large U (see Figs. 6–8).

**Expansion from a box trap: dependence on the
particle number at a fixed initial filling n_{init}**

We have also studied the dependence on the number of particles N at a fixed n_{init} . The respective results are presented in Fig. 9 for $U = 100t$ and $n_{\text{init}} = 1.8$. Qualitatively, the spatial extension and stability of the approximate Fock states grows with N . The figure further shows [see Fig. 9(d)] that by plotting the data vs τ/N , d_x/x , calculated for different N , all results collapse onto essentially the same curve. This illustrates that the time for the formation of the quasi-Fock state scales linearly with the number of particles (or the number of doublons in the initial state, respectively). Most importantly, the *qualitative* behavior of the quantum distillation process is independent of N at a fixed n_{init} .

For $n_{\text{init}} \leq 1$, no quantum distillation takes place at any U , and the dynamics in that case was studied in Ref. [8].

Radius of the double occupancies

The quantum distillation effect can be nicely illustrated by plotting the radius R_d of the double occupancies:

$$R_d^2 = \frac{1}{N_d} \sum_{i=1}^L i^2 \langle \tilde{d}_i \rangle \quad (2)$$

where $N_d = \sum_{i=1}^L \langle \tilde{d}_i \rangle$ is the total number of double occupancies. This radius is shown in Fig.10 for several values

of U and an initial density of $n = 1.8$. In this quantity, the effect is visible for $U \gtrsim 8t$.

**Expansion from the harmonic trap: Reduction of
the entanglement entropy**

Here we provide results for the reduction of the entanglement entropy for the expansion from a harmonic trap and the parameters of Fig. 4 of the main text ($V_{\text{trap}} = 0.05t$, $N = 14$, $U_{\text{init}} = 2t$), yet for two values of the interaction $U = 40t$ and $U = 100t$ after the quench. We have also performed runs with different discarded weights $\delta\rho$ to check the quality of our results. The data presented in Fig. 11(b) suggest that the reduction of the entanglement entropy is (for $x = 2, 3$ and $U = 100t$)

$$\begin{aligned} S_{x=2}(\tau) &< 0.1 S_{x=2}(\tau = 0) \\ S_{x=3}(\tau) &< 0.21 S_{x=3}(\tau = 0). \end{aligned} \quad (3)$$

Note that we have not yet reached the minimum in the time-dependent reduction of $S_x(\tau)$. At long times, the simulation is slowed down due to the relatively large entanglement of blocks with $x \gtrsim 7$. The figure unveils that the more accurate the simulation is (*i.e.*, the smaller the discarded weight), the better the efficiency of the quantum distillation in reducing $S_x(\tau)$ is captured.

The last figure, Fig. 12, illustrates the dependence of the quantum distillation on first, U [panel (a)] and second, the effective density $\tilde{\rho} = N\sqrt{V_{\text{trap}}}$ [panel (b)]. We use the parameters of Fig. 4 from the main text, except for varying U in Fig. 12(a) and varying N in Fig. 12(b). We plot the average double occupancy and we observe that similar to the case of a box trap that was discussed in the main text, quantum distillation works as long as some doublons (signified by sites with $\langle n_i \rangle > 1$ at $\tau = 0$) are present in the initial state. Also, as expected, the final U needs to be larger than $4t$ to induce the formation of a metastable state with doublons grouping together in the leftmost sites.

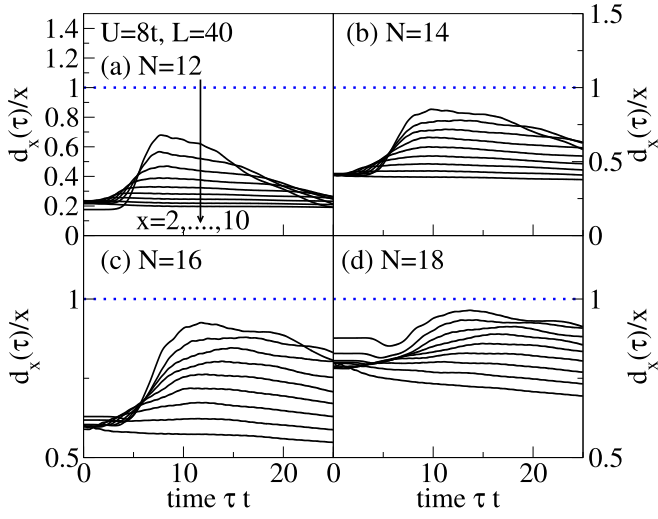


FIG. 5: (Color online) Average double occupancy $d_x(\tau)/x$ for $x = 2, \dots, 10$ ($d_x(\tau) = \sum_{i=0}^x \langle \tilde{d}_i(\tau) \rangle$) and $U = 8t$: (a) $n_{\text{init}} = 1.2$; (b) $n_{\text{init}} = 1.4$ (c) $n_{\text{init}} = 1.6$; (d) $n_{\text{init}} = 1.8$. (time step $0.01/t$, discarded weight 10^{-8}).

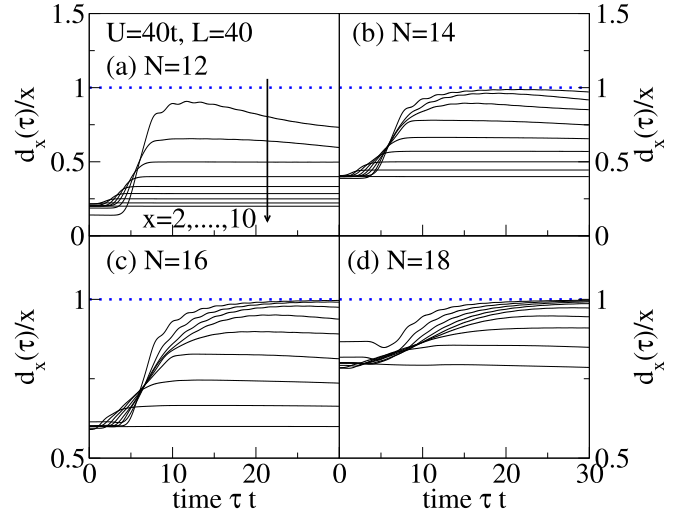


FIG. 7: (Color online) Average double occupancy $d_x(\tau)/x$ for $x = 2, \dots, 10$ ($d_x(\tau) = \sum_{i=0}^x \langle \tilde{d}_i(\tau) \rangle$) and $U = 40t$: (a) $n_{\text{init}} = 1.2$; (b) $n_{\text{init}} = 1.4$ (c) $n_{\text{init}} = 1.6$; (d) $n_{\text{init}} = 1.8$. (time step $0.01/t$, discarded weight 10^{-9}).

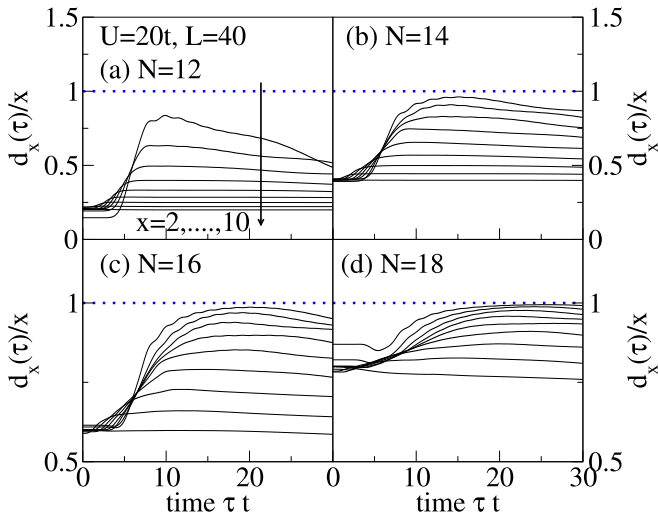


FIG. 6: (Color online) Average double occupancy $d_x(\tau)/x$ for $x = 2, \dots, 10$ ($d_x(\tau) = \sum_{i=0}^x \langle \tilde{d}_i(\tau) \rangle$) and $U = 20t$: (a) $n_{\text{init}} = 1.2$; (b) $n_{\text{init}} = 1.4$ (c) $n_{\text{init}} = 1.6$; (d) $n_{\text{init}} = 1.8$. (time step $0.01/t$, discarded weight 10^{-8}).

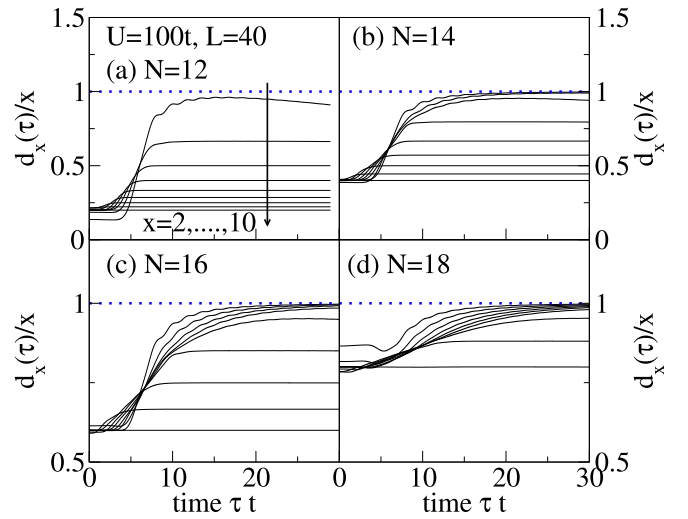


FIG. 8: (Color online) Average double occupancy $d_x(\tau)/x$ for $x = 2, \dots, 10$ ($d_x(\tau) = \sum_{i=0}^x \langle \tilde{d}_i(\tau) \rangle$) and $U = 100t$: (a) $n_{\text{init}} = 1.2$; (b) $n_{\text{init}} = 1.4$ (c) $n_{\text{init}} = 1.6$; (d) $n_{\text{init}} = 1.8$. (time step $0.01/t$, discarded weight 10^{-9}).

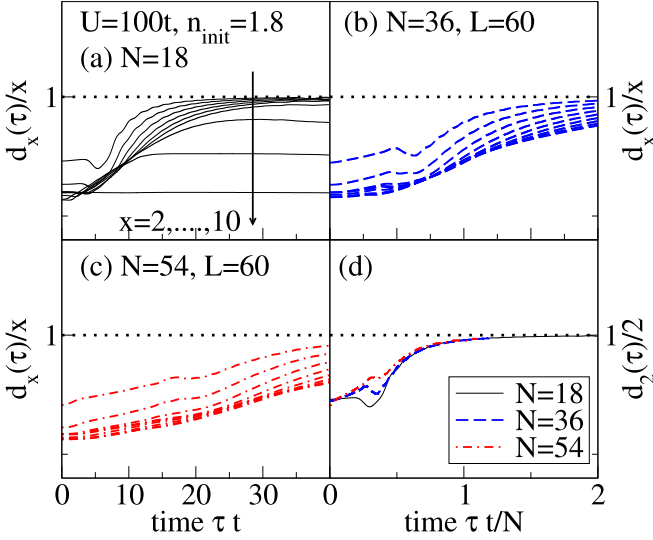


FIG. 9: (Color online) Dependence of the average double occupancy $d_x(\tau)/x$ on the number of particles at a fixed filling of $n_{\text{init}} = 1.8$ ($U = 100t$): (a) $N = 18$, $L = 40$ ($\delta\tau t = 0.01$, $\delta\rho = 10^{-9}$); (b) $N = 36$, $L = 60$ ($\delta\tau t = 0.01$, $\delta\rho = 10^{-7}$); (c) $N = 36$, $L = 60$ ($\delta\tau t = 0.02$, $\delta\rho = 10^{-7}$); (d) $d_2(\tau)/2$ vs. time τ/N (*i.e.*, rescaled on the number of particles). The same qualitative behavior is observed, independently of N . The time for building up the quasi-Fock state is simply proportional to the total number of particles. Slight differences between the results for different N at short times are due to differences in the initial state (*i.e.*, boundary and N -dependent oscillations in the density profile).

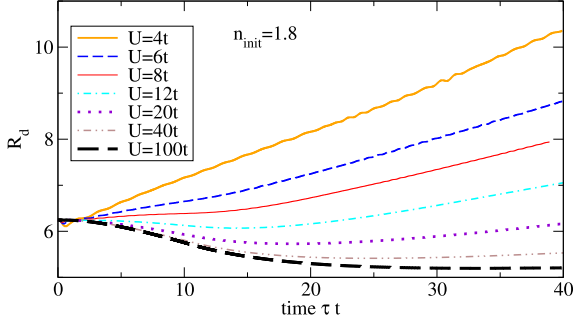


FIG. 10: (Color online) Radius R_d of the double occupancies for the expansion from a box trap with an initial density of $n = 1.8$ and several $U/t = 4, 6, 8, 12, 16, 20, 40, 100$.

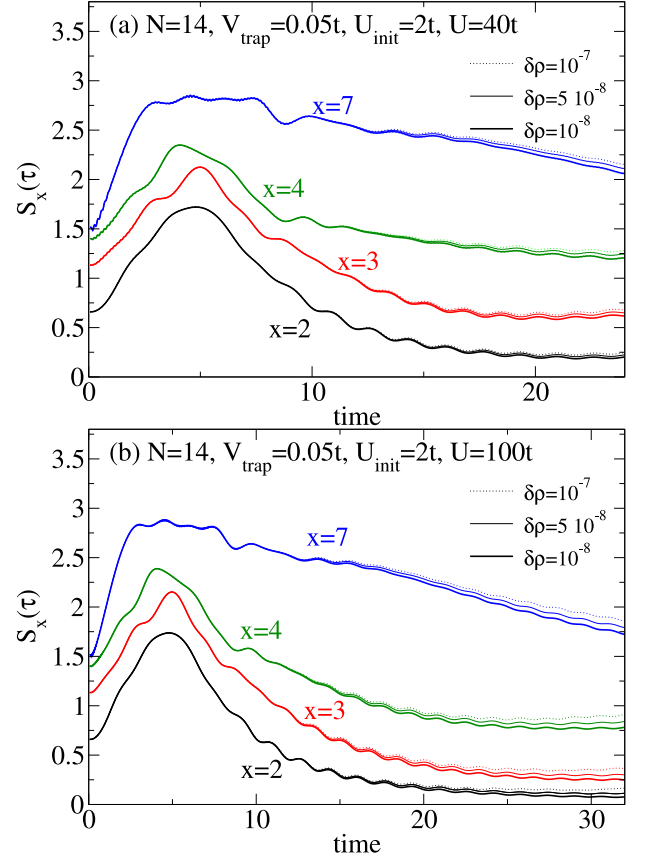


FIG. 11: (Color online) Reduction of the entanglement entropy $S_x(\tau)$ for $x = 2, 3, 4, 7$ (bottom to top) and the parameters of Fig. 4 of the main text ($V_{\text{trap}} = 0.05t$, $N = 14$, $U_{\text{init}} = 2t$): (a) $U = 40t$; (b) $U = 100t$. The runs were performed with a time step of $0.01/t$ and different discarded weights $\delta\rho$ (see the figure's legend).

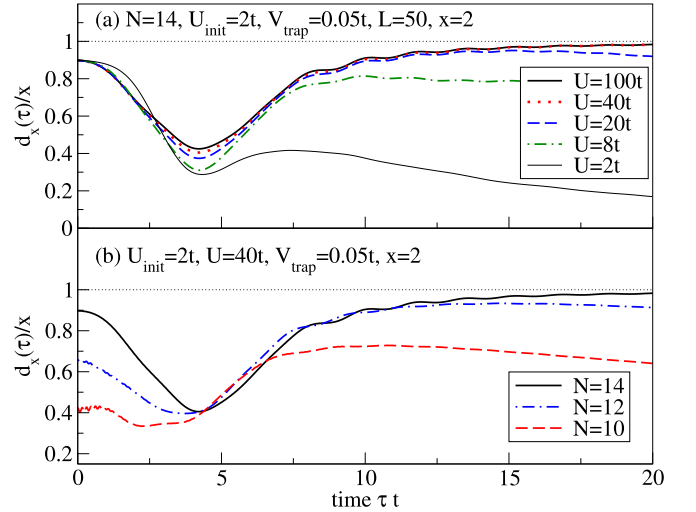


FIG. 12: (Color online) Average double occupancy $d_2/2$ for the set-up of Fig. 4 from the main text ($V_{\text{trap}} = 0.05t$, $U_{\text{init}} = 2t$) and (a) $U/t = 2, 8, 20, 40, 100$ ($N = 14$) and (b) $N = 10, 12, 14$ ($U = 40t$).